NASA TN D-1215

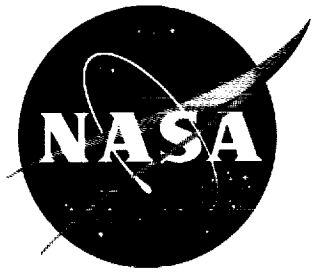

TECHNICAL NOTE

D-1215

AN ANALYTICAL AND EXPERIMENTAL EVALUATION OF A TWO-STAGE ANNULAR AIR EJECTOR FOR HIGH-ENERGY WIND TUNNELS

By John A. Sheldon and Henry R. Hunczak

Lewis Research Center
Cleveland, Ohio

NATIONAL AERONAUTICS AND SPACE ADMINISTRATION

WASHINGTON

June 1962

NATIONAL AERONAUTICS AND SPACE ADMINISTRATION

TECHNICAL NOTE D-1215

AN ANALYTICAL AND EXPERIMENTAL EVALUATION OF A TWO-STAGE ANNULAR AIR EJECTOR FOR HIGH-ENERGY WIND TUNNELS

By John A. Sheldon and Henry R. Hunczak

SUMMARY

A survey analysis was made, and cold-flow experimental tests were run to show the feasibility of using an annular two-stage air ejector in conjunction with a mechanical exhauster system to start and run a typical high-energy (~1.5 megawatt) wind tunnel. The flow conditions for the tunnel of concern are:

Stagnation enthalpy, Btu/lb	12,500
Stagnation pressure, atm	5.05
Tunnel weight flow, lb/sec	0.10
Tunnel test-section velocity, ft/sec	>20,000

The analysis was based on the properties of an inviscid real gas. Results indicate that the first-stage mass-flow ratio should be at least 100, the second-stage mass-flow ratio approximately 1, and that no major gains in performance would be obtained at ejector stagnation pressures greater than 10 atmospheres.

To proof test an axial ejector with a mass-flow ratio as high as 100, a cold-flow ejector model was tested. The minimum pressure the ejector could sustain at a given exhauster pressure was investigated with and without simulated tunnel flow bled in upstream of the ejector. The investigation was made with ejector stagnation pressures from 5.8 to 10.5 atmospheres and mixer lengths downstream of the second stage of 1.55 and 4.77 diameters. When tests were made with bleed flows, the first-stage mass-flow ratio varied between 87 and 200. The second-stage mass-flow ratio varied between 0.5 and 2.2 for all tests.

Experimental tests indicate a pressure ratio across the ejector of at least 25 could be obtained at an exhauster total pressure of at least 2.5 pounds per square inch absolute. Thus, the investigation has confirmed the ability of the ejector to operate between the maximum pressure necessary for starting a typical high-energy tunnel and the minimum pressure required to enable the exhausters to pump the combined tunnel and ejector mass flow.

INTRODUCTION

In order to simulate reentry stagnation heat transfer, a high-energy source for heating the working fluid is required (refs. 1 and 2). Consequently, in recent years a great deal of attention has been focused on the electric arc as a possible high-energy source for aerodynamic and thermodynamic experimentation. With an electric arc it appears possible to produce stagnation enthalpies of the order of 10,000 Btu per pound. A complicating factor, however, is that, to simulate high-altitude reentry stagnation conditions accurately, gas velocities of the order of 20,000 feet per second are needed. In order to simulate these velocities a high tunnel pressure ratio is necessary so that the tunnel stagnation intrinsic energy may be converted to test-section kinetic energy. Because of the necessity of a high tunnel pressure ratio, it is apparent that one of two conditions must be satisfied: (1) a high stagnation pressure (of the order of 20 atm) and a moderate test-section pressure, or (2) a moderate stagnation pressure (of the order of 5 atm) and a low test-section pressure. However, high stagnation pressures create nozzle heat-transfer and electric-arc discharge problems, and therefore the second pressure condition is the one of interest in this investigation. It is apparent then that a low discharge pressure is of interest for reentry simulation facilities of the electric-arc-tunnel type.

An effective means of obtaining a low discharge pressure has been one of the major problems facing the developers of arc-heated wind tunnels suitable for reentry heat-transfer simulation. Of the three possible ways of obtaining the proper exhaust conditions, only two are practical - vacuum tanks and ejectors. Exhausters alone have been ruled out since they are limited in the minimum pressure level attainable. The vacuum tank has two major drawbacks: (1) short running time, which is not desirable for certain types of experiment and (2) a heat exchanger, which is required to reduce the heat content of the working fluid. This now leads to the possibility of using an exhauster system preceded by an ejector system. Further, if mixing is good, the cooling requirements of the exhauster system have been minimized.

The abovementioned combination system (ejector plus exhausters) has four advantages over the other two systems:

(1) It has no limit on its running time, an obvious advantage over the vacuum tank.

(2) Its vacuum capabilities, although limited, are better than those for exhausters alone.

(3) Because of the high ejector mass-flow rate, the hot-arc tunnel exhaust is diluted, and the heat-transfer effects on the downstream components are greatly reduced or eliminated entirely.

(4) A reduction in the starting and running pressure ratios is obtained as discussed in references 3 and 4.

Thus, in general, an ejector-exhauster combination has two major advantages: First, it acts as a prolonged vacuum source; second, by diluting the arc tunnel exhaust flow the need for a heat exchanger is eliminated.

The disadvantages of the ejector-exhauster combination are the necessity of a high-pressure (up to 150 lb/sq in. abs) and high-flow (≈30 lb/sec) air source and the extremely high cost of an exhauster system, if one is not already available.

An ejector-exhauster combination system was studied both analytically and experimentally at the Lewis Research Center as to the feasibility of obtaining the vacuum necessary to operate a proposed 1.5-megawatt electric-arc tunnel. To investigate the performance of an ejector using the high mass-flow ratios required, a 1/8-scale cold-flow model was built and tested. The results are presented herein.

SYMBOLS

A	area, sq in. or sq ft
g	acceleration of gravity
h	static enthalpy, Btu/lb
J	mechanical equivalent of heat, ft-lb/Btu
L	length
M	Mach number
m	mass-flow rate, lb/sec
$\overline{m}$	molecular weight, lb/lb-mole
P	stagnation pressure, lb/sq in. or lb/sq ft abs
$\overline{P}$	average stagnation pressure, lb/sq in. or lb/sq ft abs
p	static pressure, lb/sq in. or lb/sq ft abs
R	second-stage mixer-tube length-to-diameter ratio

$\overline{R}$ universal gas constant, (ft)(lb)/(lb-mole)(^{o}R)

Re Reynolds number

r_1 $\dfrac{\text{First-stage ejector mass flow}}{\text{Arc tunnel mass flow}} = \dfrac{m_{j1}}{m_b}$

r_2 $\dfrac{\text{Second-stage ejector mass flow}}{\text{First-stage ejector mass flow + Arc tunnel mass flow}} = \dfrac{m_{j2}}{m_{j1} + m_b}$

r_{1+2} $\dfrac{\text{Second-stage mass flow + First-stage mass flow}}{\text{Arc tunnel mass flow}} = r_2(r_1 + 1) + r_1$

T temperature, ^{o}R

u velocity, ft/sec

δ ejector throat distance, in.

ρ density, slugs/cu in. or lb/cu ft

Subscripts:

b bleed flow

e blank end (ejector tube inlet)

fs full-scale ejector

i ejector tube inlet

j ejector

j1 first-stage ejector

j2 second-stage ejector

j1,2 both ejector stages

M mixed flow

P pilot ejector

R rake (exhauster)

Superscript:

* ejector throat area

OPERATIONAL CONSIDERATIONS

Since the pressure ratio across the tunnel circuit is slightly higher for starting than for steady-state operation, the experiment and theory were concerned with the starting operation. During the starting operation the ejector-exhauster system must create static pressures low enough to pull the shock configuration from the tunnel nozzle and test section into the diffuser section. Consequently, the tunnel flow into the ejector system will be subsonic in the starting case and become supersonic during steady-state operation. The purpose of the ejector is then to pump the tunnel flow from a low static pressure behind the starting normal shock to a high total pressure downstream so that the exhausters can operate satisfactorily.

Theoretical and experimental studies of the performance and operation of ejectors can be found in references 3 to 6. However, these results are limited in their usefulness to ideal gases; and, since real-gas effects were of importance, a new study was deemed necessary. Consequently, an exploratory analytical study was made to determine the feasibility of using ejectors in conjunction with conventional exhaust facilities. Of particular interest was the maximum pressure to which the ejector could pump the tunnel free-stream flow for a given tunnel stagnation enthalpy, stagnation pressure, and mass flow. It was also desired to determine the number of stages needed and where the practical operation conditions would exist. In general, the analysis was made to show the trends and ranges of design parameters. Its purpose was not intended to compare theory and experiment. An outline and discussion of the analytical study are given in the appendix.

From the theoretical analysis the following design criteria were established:

(1) Two ejector stages

(2) Ejector stagnation pressures of about 10 atmospheres

(3) First-stage mass-flow ratio r_1 of 100 or more

(4) Second-stage mass-flow ratio r_2 of about 1

TEST APPARATUS AND PROCEDURE

Design of the experimental model was based on the arc tunnel flow conditions selected from a detailed study made at the NASA Lewis Research Center. These conditions are listed as follows:

Stagnation enthalpy, H, Btu/lb	12,500
Stagnation pressure, P, atm	5.05
Tunnel mass flow, m, lb/sec	0.10
Tunnel test-section velocity, u, ft/sec	21,125
Tunnel test-section Mach number, M	5.3
Tunnel test-section static pressure, p, atm	0.0005
Static pressure behind test-section shock, p_e, lb/sq in. abs	0.136

Description of Model

Because of the high temperatures encountered in the arc tunnel and the desirability of not obstructing the airflow, annular injection was picked over the more conventional center injection.

A detailed drawing of the 1/8-scale ejector configuration investigated is shown in figure 1. The nozzle throat size and consequently the exit- to inlet-area ratio of both stages could be changed by means of the three setscrews. The ejector throat distances were determined by using calibrated shims. Care was taken in retaining symmetry of the annular ejector nozzle contour.

Reference 4 shows that the 10° entry angle facilitates the mixing of ejector flow and mainstream flow, and therefore a 10° entry angle was used in this investigation.

The two-stage ejector system was mounted vertically as shown in figures 2 and 3. Airflow to simulate the tunnel flow was bled from the room through the blank end of the ejector. The flow rate was measured by means of a rotameter. To ensure obtaining a diffuse low-velocity flow that would fill up the entire flow area, a deflector plate was inserted over the bleed flow inlet.

The main ejector mass flow was introduced into both ejector stagnation cavities by four 1/4-inch inlets. The flow was regulated by two hand valves (one for each stage) shown in figure 3.

Variation of the downstream exhaust pressure was obtained by throttling the 12-inch gate valve shown in figure 2.

Instrumentation

Pressure readings were taken at the following locations:

Blank end. - Three static-pressure taps were located at different circumferential positions around the center bleed hole. Throughout all

the runs the three pressures were almost identical, therefore indicating axial symmetry at this location.

Ejector stagnation chamber. - One pressure reading for each stage was taken from a precision pressure gage (see fig. 4). Accuracy of the gage was within ±1/2 pound per square inch.

Ejector nozzle exit. - Four static-pressure taps for each stage were located 90° apart circumferentially around the ejector nozzle exit. Besides indicating the exit static pressure these static taps also gave an indication of flow symmetry.

Ejector tube exit. - A pressure rake was located downstream of the ejector at the end of the diffuser. The rake has six total-pressure probes and one static-pressure probe. The total-pressure probes are located radially in such a position that each probe surveys an equal cross-sectional area. Therefore, an average of the readings would give the bulk total pressure of the flow at this axial location.

The three pressures at the blank end and the eight pressures at the ejector nozzle exit were read on an absolute oil manometer board. The downstream pressure rake was connected to a mercury manometer board. Accuracies read were within ±0.05 inch. A photograph of the manometer board and related equipment is shown in figure 4.

Ejector mass-flow rates were calculated from the known stagnation-pressure and throat areas. Rake total pressures were corrected in the supersonic cases for the true stream total pressures using reference 7. After corrections were made, the readings of the five probes were averaged to obtain $\bar{P}_R$. Local Mach numbers at the rake were obtained using reference 7 and the measured static- to total-pressure ratio.

Procedure

The range of the test variables was as follows:

(1) Ejector stagnation pressure: 85 to 155 pounds per square inch

(2) Ejector throat dimension:

First stage:

$\delta_{j1} = 0.006$ in. $\quad \left(\frac{A}{A^*}\right)_{j1} = 44.5$

$\delta_{j1} = 0.008$ in. $\quad \left(\frac{A}{A^*}\right)_{j1} = 37.4$

Second stage (for all tests):

δ_{j2} = 0.006 in. $\left(\frac{A}{A^*}\right)_{j2}$ = 9.65

(3) Second-stage mixer-tube length:

Long mixer tube: R = 4.77

Short mixer tube: R = 1.55

(4) Bleed flow, 0 and 0.0016 pound per second

For a given ejector stagnation pressure, throat setting, and bleed flow runs were made by varying the ejector exhaust pressure with the downstream gate valve. Tests were then repeated for different ejector stagnation pressures, two different first-stage throat distances, and two bleed flows.

Runs were started with the downstream gate valve wide open. Data were then taken for various valve settings. As the valve was closed, a point was reached where a sudden surge in the blank-end pressure was observed. The valve position just preceding the surge point is defined as the "minimum-run" point. Data beyond the minimum-run point are defined as "flow-lost" points. This procedure was then reversed until the blank-end pressure returned to its previous low value. This point is defined as the "minimum-start" point.

RESULTS AND DISCUSSION

Results of typical test runs are shown in figure 5. It is apparent from the discontinuous character of the curves that the shock formations change discontinuously in the ejector tube and thus affect the ejector blank-end pressure. Although it was impossible to observe the shock pattern during the experiment, the following explanation of the flow process satisfies the experimental results.

An explanation of the flow process may be made with the help of figure 6. As previously mentioned, the test is started with the gate valve wide open. (In subsequent discussions this will be referred to as the "open-run" point.) Throttling the gate valve causes the ejector exhaust static pressure to increase and a region of transition from supersonic to subsonic flow to proceed upstream. For simplicity this region will, from now on, be depicted as a normal shock. The shock pattern moves past the rake (fig. 6) and causes the sudden decrease in corrected total pressure P_R observed in figure 5. (For lower stagnation-pressure runs this reduction in pressure did not occur,

indicating that the shock was upstream of the pressure rake at all points observed.) A further increase in the downstream pressure causes the shock to proceed up through the supersonic diffuser. Because of the decrease in the shock Mach number, the total pressure increases as the shock proceeds upstream. As the shock progresses farther upstream, the second-stage ejector is affected. A sharp increase in the second-stage ejector exit pressure was noted at this point during all the runs. With further throttling, a point is finally reached where the normal shock becomes an oblique shock at the ejector nozzle exit. At this point the flow no longer mixes in the center of the ejector tube, but tends to "cling" to the tube walls. Experimental evidence of this will be shown later. As a result, a region of low-energy air develops in the center of the tube, and the high pressure feeds back to the upstream blank end (see C of fig. 6). This increase in the blank-end pressure is sudden and discontinuous, and the point just preceding this increase (B of fig. 6) is the minimum-run point. In other words, the minimum-run point is the maximum exhaust pressure that the ejectors can produce and yet satisfactorily maintain the low blank-end pressure necessary for tunnel starting. If the flow is throttled farther, the blank-end pressure will continue to rise as shown in figure 5. These points are the flow-lost points. At any arbitrary flow-lost point the procedure may be reversed (i.e., the gate valve is opened), and the blank-end pressure will decrease. Eventually, as the gate valve is opened, the oblique shock at the ejector nozzle exits will suddenly become a normal shock in the main ejector tube. At this point the blank-end pressure has returned to its previous low value and is the minimum-start point.

The minimum-start point is the first point at which the ejector will produce the low blank-end pressure when started from a flow-lost condition. Consequently the minimum-start point is of major interest, since this point sets the maximum pressure at which the exhausters can operate and still start the ejector. The minimum-run point is of secondary importance because it represents the maximum pressure at which the exhauster can operate after the ejector has been started (i.e., after the ejector system has reached the low blank-end pressure). It would be meaningless to speak of a minimum-run point if the exhausters were unable to operate at a pressure ($\overline{P}_R$) low enough to achieve the minimum-start point.

The close proximity of the minimum-start and minimum-run points is apparent in figures 7(a) to (c). Slight differences in the pressures can be mostly accredited to viscous effects on the shock motion. However, because of flow instabilities the pressure differences are within the experimental error of this investigation, and therefore the minimum-run and minimum-start points may be assumed to be identical.

The summary curves of figure 7 show the effects of changing the ejector stagnation pressure on p_e and $\overline{P}_R$ at a constant ejector exit

Mach number. As expected, an increase in both p_e and $\overline{P}_R$ with $P_{j1,2}$ is indicated. A slight dip in the p_e curves is noted in a couple cases. This irregularity is probably due to experimental error.

Comparison of figure 7(a) with 7(c), and figure 7(b) with 7(d), shows the effects of an increase in the first-stage mass-flow rate at constant stagnation pressure on ejector performance for the zero- and 0.0016-pound-per-second bleed-flow runs, respectively. Typical results are summarized in the following table:

δ_{j1}, in.	Minimum run		m_{j1}, lb/sec
	p_e, lb/sq in. abs	$\overline{P}_R$, lb/sq in. abs	
$P_{j1,2}$ = 142 lb/sq in. abs; m_b = 0; δ_{2j} = 0.006 in.			
0.008	0.067	3.1	0.28
.006	.045	2.6	.23
$P_{j1,2}$ = 142 lb/sq in. abs; m_b = 0.0016 lb/sec; δ_{2j} = 0.006 in.			
0.008	0.087	2.95	0.28
.006	.066	2.50	.23

An increase in p_e and $\overline{P}_R$ is noted for the higher mass-flow cases. Most of the experimental tests were run at the δ_{j1} = 0.006 inch design point.

A longer second-stage mixer tube was added when it was felt that perhaps the flow was not mixing well enough after the second-stage ejector. Results, shown in figures 7(d) and (f) and summarized in the following table, tend to verify this in the bleed-flow case:

Mixer tube	R	$\overline{P}_R$, minimum run, lb/sq in. abs
$P_{j1,2}$ = 142 lb/sq in. abs; m_b = 0		
Short	1.55	2.6
Long	4.77	2.6
$P_{j1,2}$ = 142 lb/sq in. abs; m_b = 0.0016 lb/sec		
Short	1.55	2.5
Long	4.77	3.1

Tests with and without bleed flow were made to compare the bleed-flow effects on the ejector performance. The results show an increase in p_e of 20 to 50 percent for $m_b = 0.0016$ pound per second. Although there was little change in $\overline{P}_R$ for the short mixer tube, the long mixer tube showed an increase in $\overline{P}_R$ of approximately 20 percent for the bleed-flow case.

Curves of local Mach number at the rake against distance from ejector tube center are plotted in figure 8. The Mach number gives an indication of the velocity at a particular radius from the ejector tube center. Examination of figures 8(a) and (b) indicates what appears to be fully developed pipe flow for the open- and minimum-run conditions. However, the flow-lost profiles show a low velocity at the center with higher velocities closer to the wall, thus verifying the previous discussion about the central low-energy region. Figure 8(c) plots the Mach profile for a high-stagnation-pressure run with the extended mixer tube added. The open run has a Mach number of 2 at the tube center. For the minimum run the shock system is upstream of the pressure rake, and the Mach number is correspondingly subsonic. The Mach number at the center of the tube is now about 0.4. Examination of the flow-lost profile for this case shows a more uniform profile than previously observed. The added mixing length has undoubtedly been a big factor in obtaining this profile.

Because of the close proximity of the gate valve to the pressure rake, and also because of the unsymmetric nature of the nearly closed gate valve, it was felt that the flow could be separating upstream of the pressure rake. During the tests several reruns were made using a butterfly valve located much farther downstream. Favorable comparison of the results indicates that the gate valve had little or no adverse effects on the upstream instrumentation.

The bleed-flow test was made to simulate the tunnel starting flow because an arc tunnel of the proper size was not immediately available and also to simplify the experiment as much as possible. Since the mass-flow ratio of the first ejector stage is so high ($r_1 = 150$), high-temperature effects from the hot tunnel flow on most of the ejector tube length are assumed to be small. A brief qualification of this assumption follows.

The full-scale ejector, when used in conjunction with the electric-arc tunnel previously mentioned, will have a total temperature of 850° R after complete first-stage mixing. This compares to the 520° R total temperature of the pilot ejector. After second-stage mixing the total temperature drops to 700° R compared, again, with the pilot ejector's total temperature of 520° R.

When comparing temperature effects on ejector performance, two important parameters to consider are the Reynolds and Mach numbers. The Reynolds number is important since it gives an indication of viscous pressure losses, while the Mach number gives an indication of the normal shock losses.

The Reynolds number ratio of the full-size ejector to the pilot ejector is approximately given by the following:

$$\frac{Re_{fs}}{Re_P} = \frac{L_{fs}}{L_P}\left(\frac{T_P}{T_{fs}}\right)^{0.76}$$

where L is the characteristic length. Since $L_{fs} = 8L_P$ for the ejector configuration,

$$\frac{Re_{fs}}{Re_P} = 8\left(\frac{T_P}{T_{fs}}\right)^{0.76}$$

If T_P/T_{fs} is taken as 520/850, the Reynolds ratio is 5.5, indicating a considerably higher relative Reynolds number for the full-scale ejector and a higher resulting pressure recovery. Past experience with supersonic wind tunnels has justified this viewpoint.

It appears that the shock pressure losses in the hot-flow ejector will be somewhat higher than the ejector model tested because the hot-flow Mach number is higher. However, this effect is not expected to override the favorable scale effect, and an overall increase in the performance of the full-scale, hot-flow ejector is anticipated.

SUMMARY OF RESULTS

Pressure measurements were made on a 1/8-scaled pilot air ejector. Room air was bled through the upstream end of the ejector to simulate an arc tunnel starting flow. Tests were made by varying the exhaust pressure by means of a throttled exhaust valve. Runs were repeated for different ejector stagnation pressures, two different first-stage throat distances, zero bleed flow, and two different second-stage mixer-tube lengths. Mach number profiles were made to help explain a possible flow process that would satisfy the experimental observations.

In general the experimental results show the feasibility of using a two-stage air ejector in conjunction with a mechanical exhauster system to establish the pressure level required to start a high-energy supersonic wind tunnel. The specific final results may be summarized as follows:

1. With the ejector design condition (ejector stagnation pressure = 10 atm, ejector throat dimension = 0.006 in.) an upstream static pressure of 0.09 pound per square inch absolute and an exhauster pressure of 3 pounds per square inch absolute can be obtained. This is within the limit necessary for arc tunnel starting with the existing exhauster system.

2. Generally the experimental results show an increase in upstream static pressure and exhauster pressure with ejector stagnation pressure.

3. The extended second-stage mixer tube increased the exhauster pressure by 20 percent for the bleed-flow case, and mixer tubes of at least this length-to-diameter ratio (4.77) probably should be used in future designs.

4. A 33-percent increase in the first-stage throat dimension increased the upstream static pressure by 32 percent and the exhauster pressure by 18 percent for the bleed-flow case.

5. A 0.0016-pound-per-second bleed flow changed the exhauster pressure slightly but increased the upstream static pressure by 20 to 50 percent. Even so, the pressure measurements are still within the range required for starting a typical reentry simulating facility.

Lewis Research Center
National Aeronautics and Space Administration
Cleveland, Ohio, February 13, 1962

APPENDIX - THEORETICAL ANALYSIS

An analysis to determine the general performance trends of a two-stage ejector was conducted prior to the selection of the final arc tunnel design specifications. For this analysis the following preliminary tunnel flow conditions were used:

Stagnation enthalpy, Btu/lb	12,500
Stagnation pressure, atm	7.6
Free-stream velocity, ft/sec	21,240
Weight flow, lb/sec	0.16

Assumptions

As is usually done for simplicity in exploratory surveys of this type, chemical equilibrium and one-dimensional flow were assumed throughout with the specification that the flow mixing process occurs either at constant area or constant pressure. Furthermore, boundary-layer effects were neglected.

Equations

Basic equations used in the analytical evaluation were as follows:

Continuity:

$$\rho_i u_i A_i + \rho_j u_j A_j = \rho_M u_M A_M$$

Momentum:

$$\frac{m_i u_i}{g} + p_i A_i + \frac{m_j u_j}{g} + p_j A_j = \frac{m_M u_M}{g} + p_M A_M$$

Energy:

$$h_j + \frac{1}{2}\frac{u_j^2}{gJ} + h + \frac{1}{2}\frac{u_i^2}{gJ} = h_M + \frac{1}{2}\frac{u_M^2}{gJ}$$

State:

$$\frac{P}{\rho} = \frac{\bar{R}}{\bar{m}} T$$

In addition, constant area mixing was used; therefore,

$$A_i + A_j = A_M$$

Procedure

The extremely high stagnation enthalpy required the use of real-gas charts (ref. 8). Graphical solutions for the free-stream flow, normal shock, and flow mixing process in the first stage were used as there are no explicit solutions to the energy, momentum, and continuity equations.

The tunnel stagnation conditions, weight flow per unit area and the free-stream velocity, are all the quantities necessary to calculate the tunnel flow conditions and those of the normal shock. It was then stipulated that, for starting, the static pressure of the supersonic flow from the first ejector stage be equal to that behind the free-stream normal shock. Subsonic and supersonic solutions were obtained for the mixed flow. For entrance conditions to the second stage the subsonic solution of the mixed flow was used. As with the first stage, the static pressure of the supersonic flow from the second stage was set equal to that of the mixed flow entering it. When possible, calculations for the second stage were made using an average value of the specific-heat ratio and flow tables such as those of references 7 and 9.

The ejector variables studied are listed as follows:

First stage	
Stagnation pressure, P_{j1}, atm	10, 20, and 30
Stagnation temperature, T_{j1}, ^{o}R	530
Tunnel-to-ejector mass ratio, r_1	1, 2, ≈ 75, 100, 150, and 200
Second stage	
Stagnation pressure, P_{j2}, atm	$= P_{j1}$
Stagnation temperature, T_{j2}, ^{o}R	530
Tunnel-to-ejector mass ratio, r_2	1 and 100

First-stage ejector performance as a function of mass ratio is plotted in figure 9. From a mass ratio r_1 of 2 to 75 no flow mixing solutions existed. This lack of solutions corresponds to choking of the combined flow by the high heat content of the tunnel flow. The choking limits as a function of ejector total pressure were not well defined because of the limited accuracy in reading the Mollier charts. A substantial improvement in the running pressure (supersonic mixed flow curves) over the starting pressure (subsonic mixed flow curves) can be noted as

the mass ratio is increased. Single-stage ejector performance as a function of ejector stagnation pressure is shown in figure 10. The major increase in performance at all mass-flow ratios was obtained at or before a stagnation pressure of 10 atmospheres.

Using two stages with a mass ratio r_1 of 100 in stage one and $r_2 = 1$ in stage two improved the downstream stagnation pressure by approximately 13 percent over injecting all the flow in a single stage. The overall mass ratio r_{1+2} was 201. Reversing the mass ratios, that is, $r_1 = 1$, $r_2 = 100$, gave no improvement over injecting all the flow in a single stage. This is indicated by the datum point. An additional benefit of using a high mass ratio in the first stage is that the relatively cool ejector flow immediately blankets and dilutes the tunnel flow to an average temperature of approximately 850° R, which is well within the temperature limits of structural materials, thus greatly reducing the cooling requirements.

The analysis and flow capacity of existing pumping equipment indicate the use of a two-stage ejector. The mass ratio of the first stage should be at least 100, that of the second stage approximately 1.0; and no major gains in performance may be expected by increasing the ejector stagnation pressure above 10 atmospheres.

As previously stated, all test-section conditions have been based on equilibrium flow expansion. It is realized that this assumption is not strictly valid and that the flow process actually freezes at some point in the expansion process. Additional calculations were made based on the opposite extreme assumption that the expansion process is frozen at stagnation conditions. Results have shown a test-section static pressure of about 1.9×10^{-5} atmosphere and a test-section Mach number of about 17.2. Although these numbers are considerably different from their equilibrium counterparts quoted on page 6 ($P = 0.0005$ atm, $M = 5.3$), the static pressure behind the test-section normal shock in the frozen flow is about 0.10 pound per square inch absolute. This pressure is reasonably close to 0.136 pound per square inch absolute for the equilibrium condition. It is felt that in the real case the starting pressure behind the tunnel shocks will lie somewhere between these values, and therefore the analysis should be valid.

REFERENCES

1. Palmer, George M.: A Study of the Overall Problems of the True-Temperature, Hypersonic Wind Tunnel Having Semi-Continuous Operation and the Preferred Method of Solution. Rep. A-59-14, Purdue Univ., Aug. 1959.

2. Stalder, Jackson R., Goodwin, Frederick K., Ragent, Boris, and Noble, Charles E.: Aerodynamic Applications of Plasma Wind Tunnels. Rep. 18, Vidya, Inc., Feb. 29, 1960.

3. Spiegel, Joseph M., Hofstetter, Robert U., and Kuehn, Donald M.: Applications of Auxiliary Air Injectors to Supersonic Wind Tunnels. NACA RM A53I01, 1953.

4. Hunczak, Henry R., and Rousso, Morris D.: Starting and Operating Limits of Two Supersonic Wind Tunnels Utilizing Auxiliary Air Injection Downstream of the Test Section. NACA TN 3262, 1954.

5. Howell, Robert R.: Experimental Operating Performance of a Single-Stage Annular Air Ejector. NASA TN D-23, 1959.

6. Keenan, J. H., Neumann, E. P., and Lustwerk, F.: An Investigation of Ejector Design by Analysis and Experiment. Jour. Appl. Mech., vol. 17, no. 3, Sept. 1950, pp. 299-309.

7. Ames Research Staff: Equations, Tables, and Charts for Compressible Flow. NACA Rep. 1135, 1953. (Supersedes NACA TN 1428.)

8. Moeckel, Wolfgang E., and Weston, Kenneth C.: Composition and Thermodynamic Properties of Air in Chemical Equilibrium. NACA TN 4265, 1958.

9. Foa, J. V.: Mach Number Functions for Ideal Diatomic Gases. Cornell Aero. Lab., Inc., Oct. 1949.

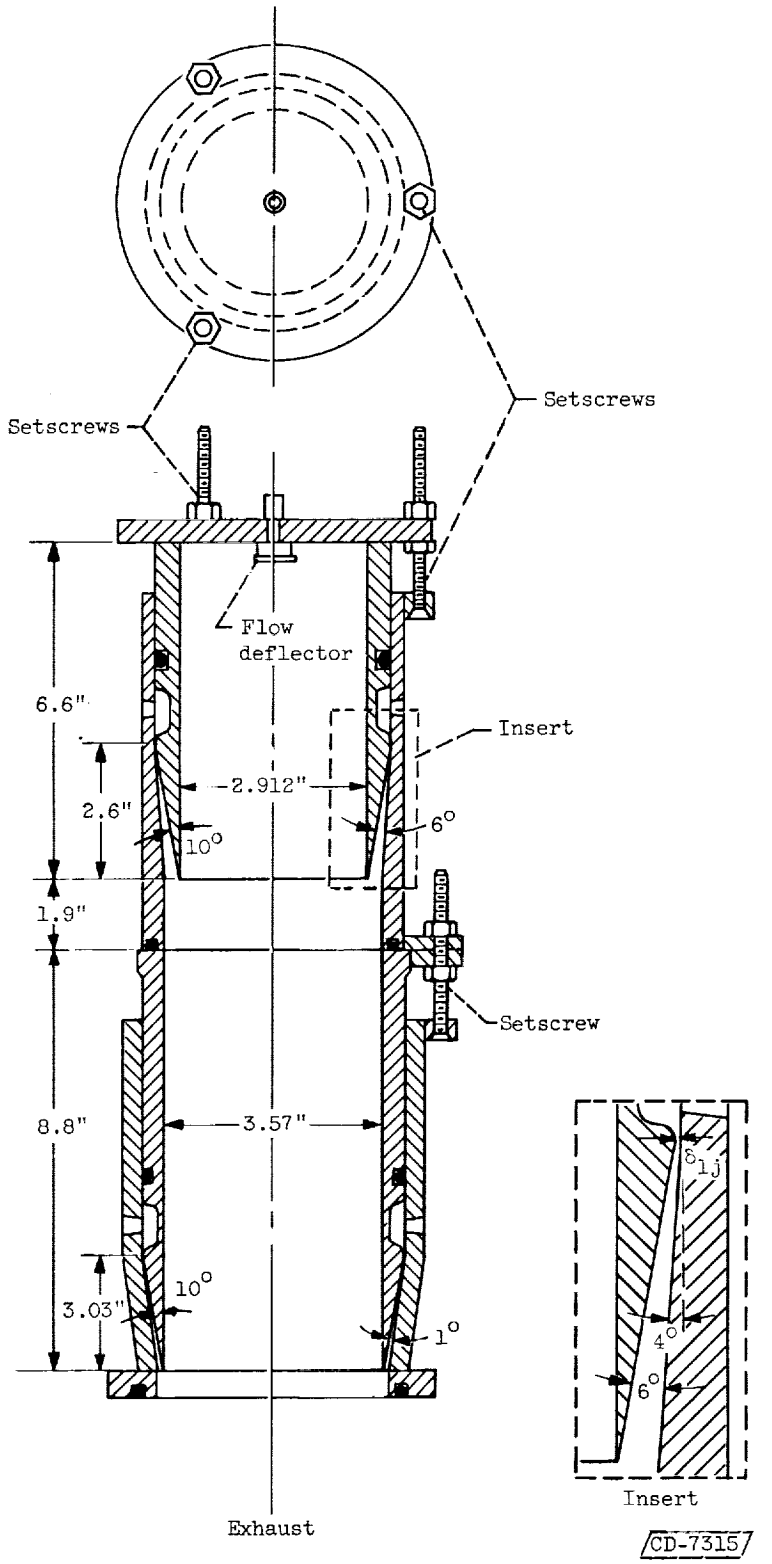

Figure 1. - 1/8-Scale ejector detail.

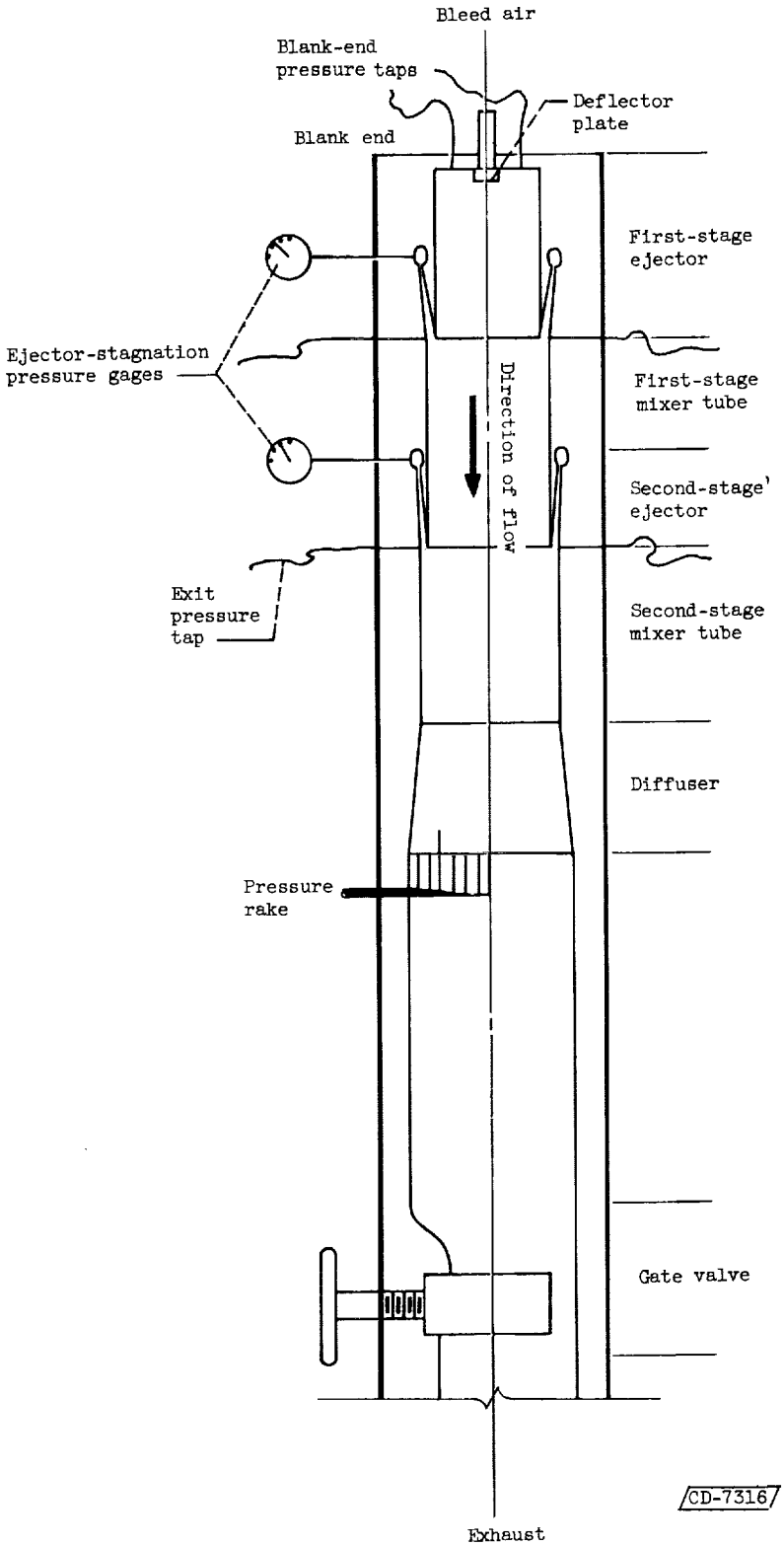

Figure 2. - Ejector schematic.

Figure 3. - Ejector installation.

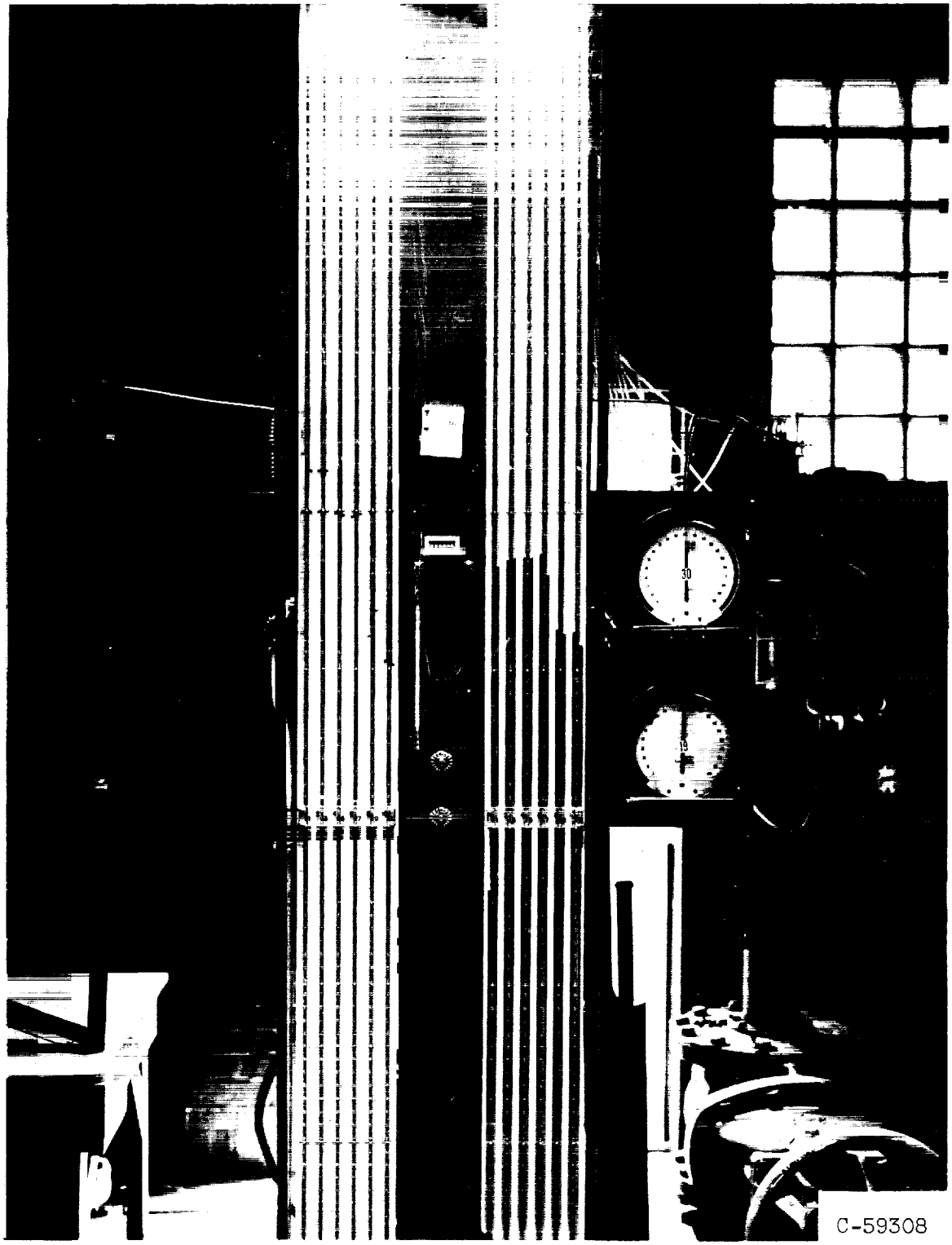

Figure 4. - Instrumental installation.

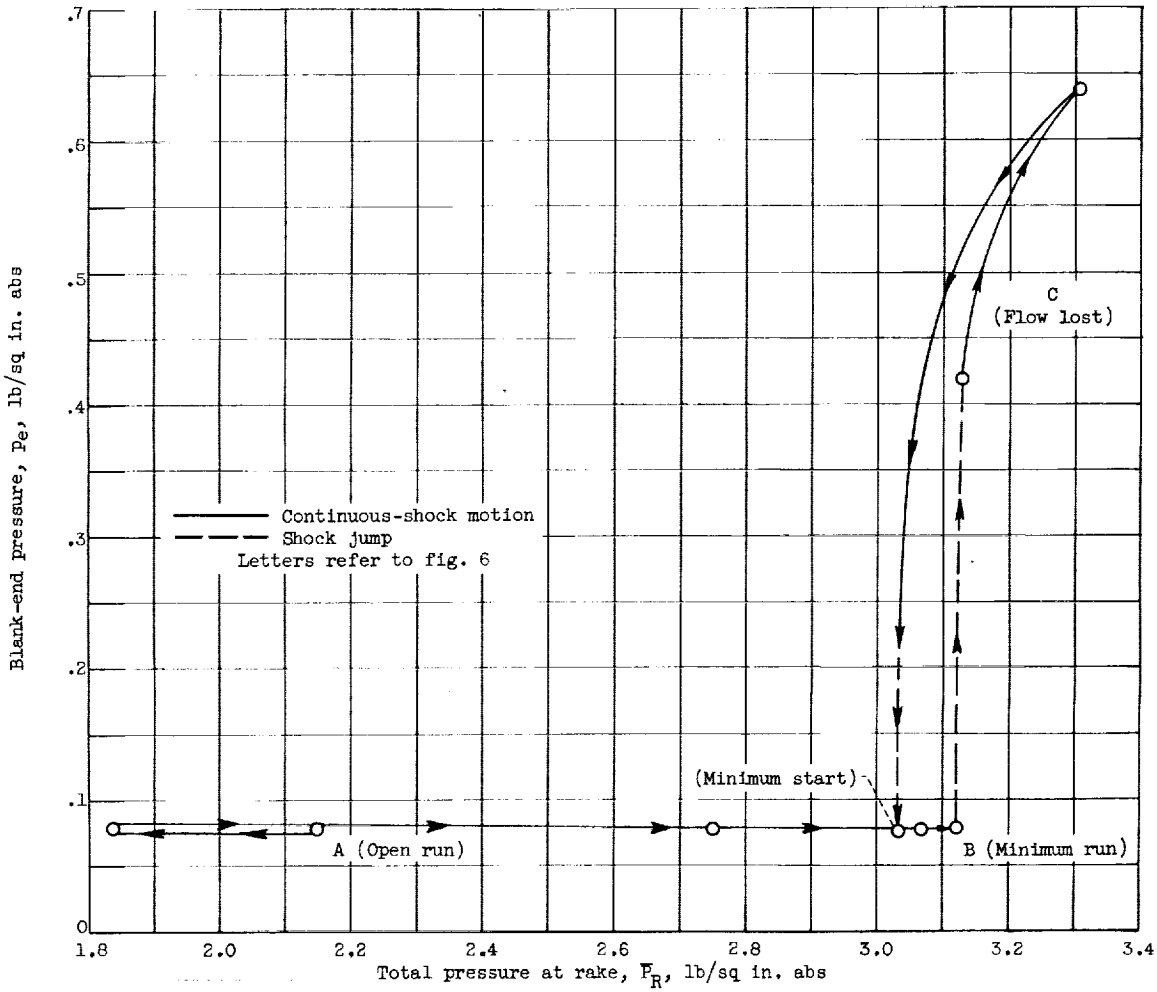

(a) First- and second-stage ejector pressure, 150.3 pounds per square inch absolute; bleed flow, 0.0016 pound per second; first-stage ejector mass flow, 0.245 pound per second; second-stage ejector mass flow, 0.296 pound per second; long mixer tube.

Figure 5. - Ejector hysteresis curves.

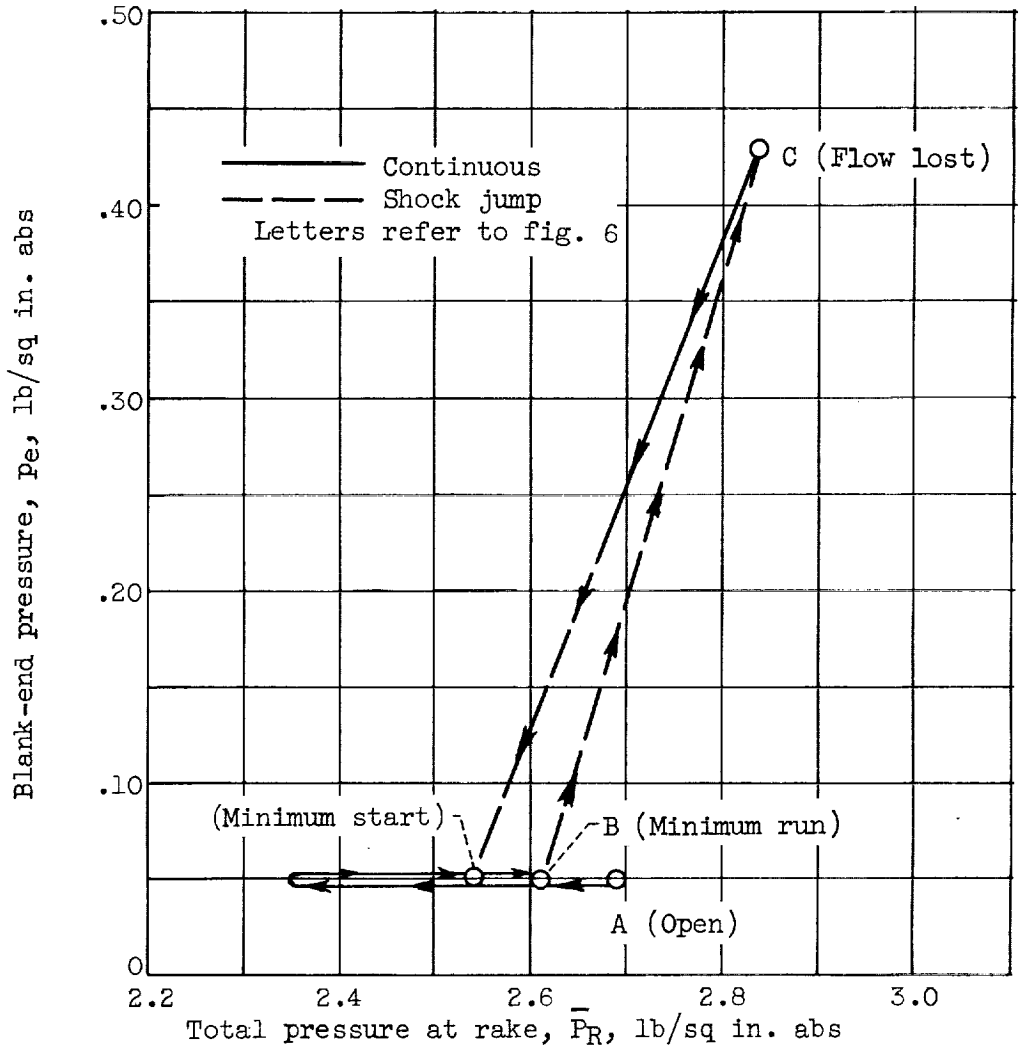

(b) First- and second-stage ejector pressure, 146.5 pounds per square inch absolute; no bleed flow; first-stage ejector mass flow, 0.239 pound per second; second-stage ejector mass flow, 0.287 pound per second; short mixer tube.

Figure 5. - Concluded. Ejector hysteresis curves.

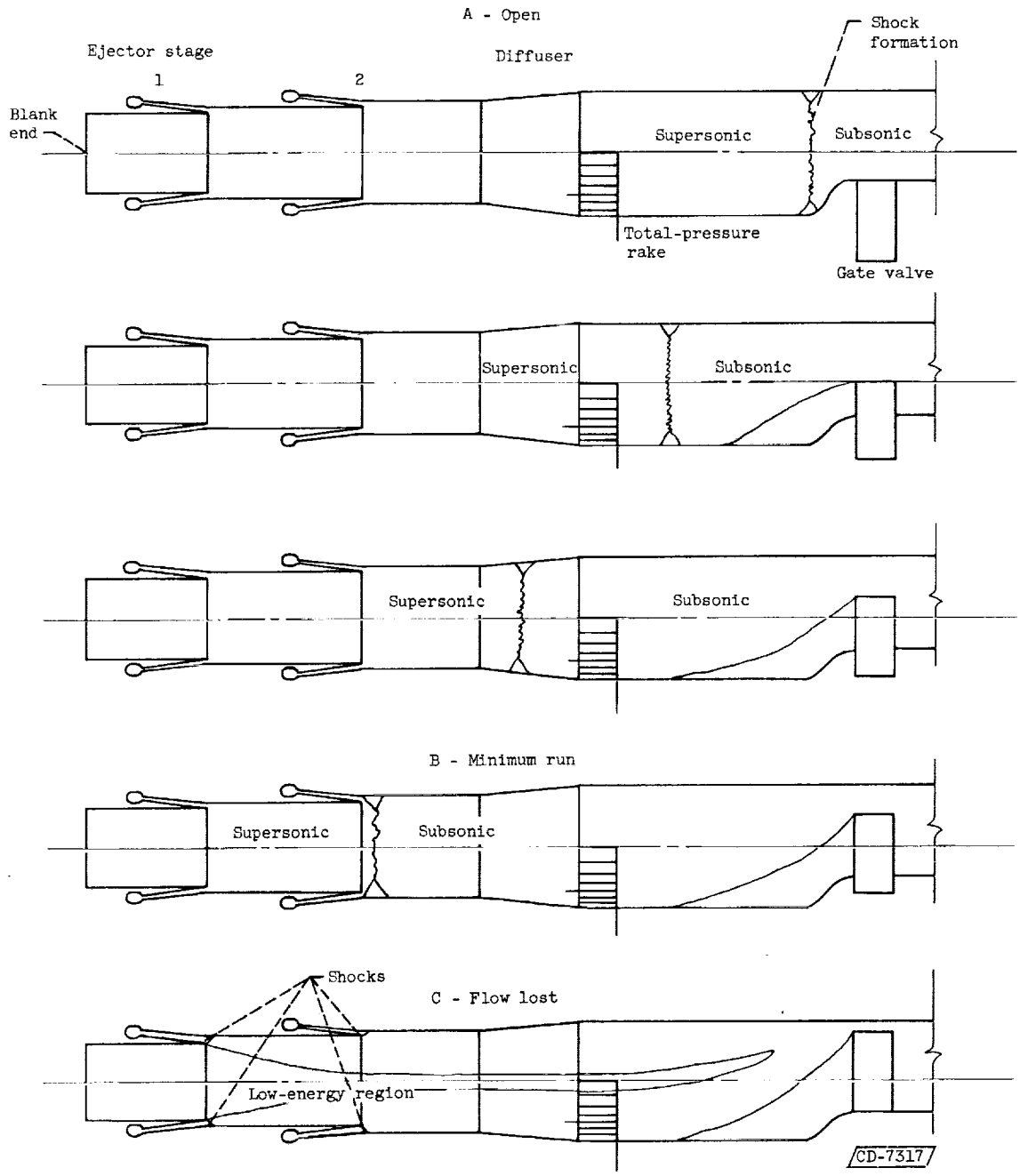

Figure 6. - Flow configurations.

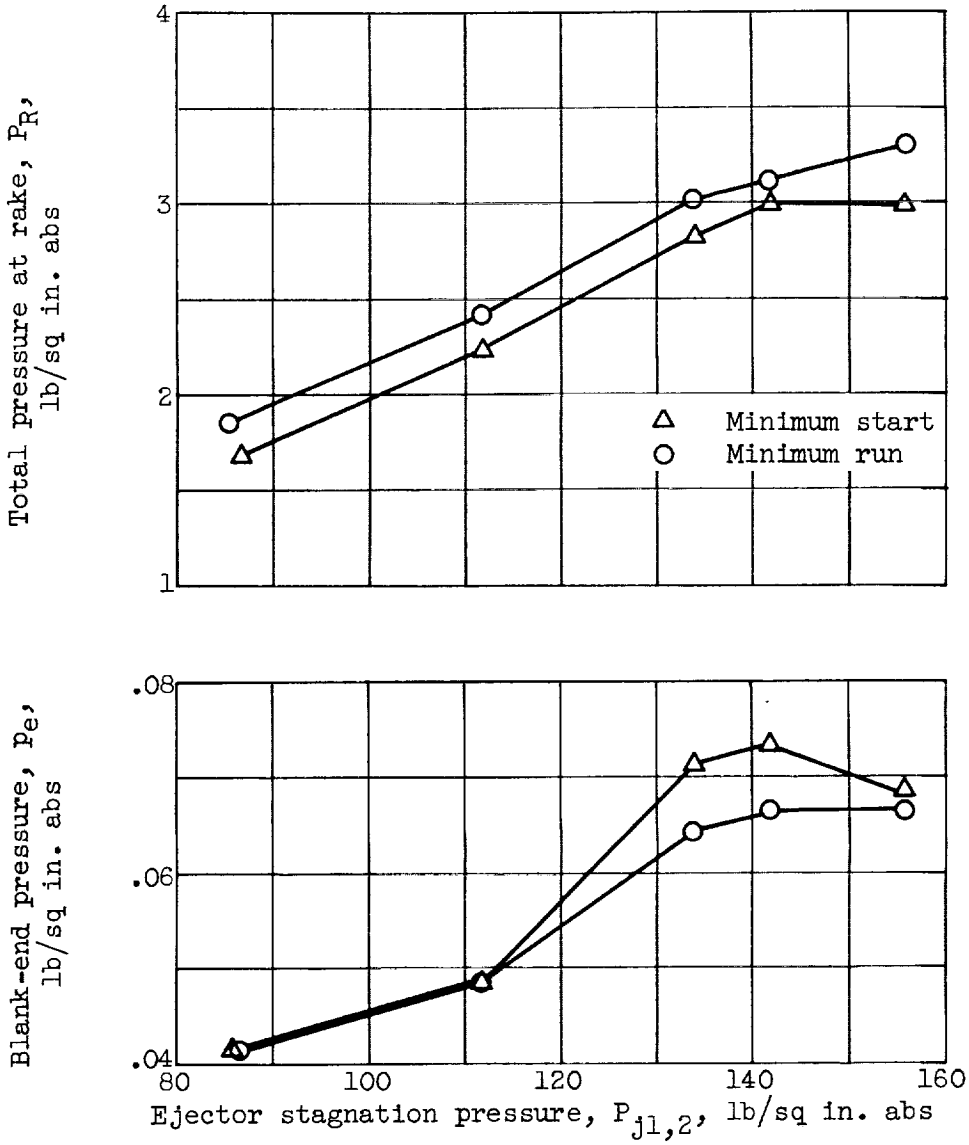

(a) No bleed flow; first-stage ejector throat distance, 0.008 inch; short mixer tube.

Figure 7. - Summary curves. Second-stage ejector throat distance, 0.006 inch.

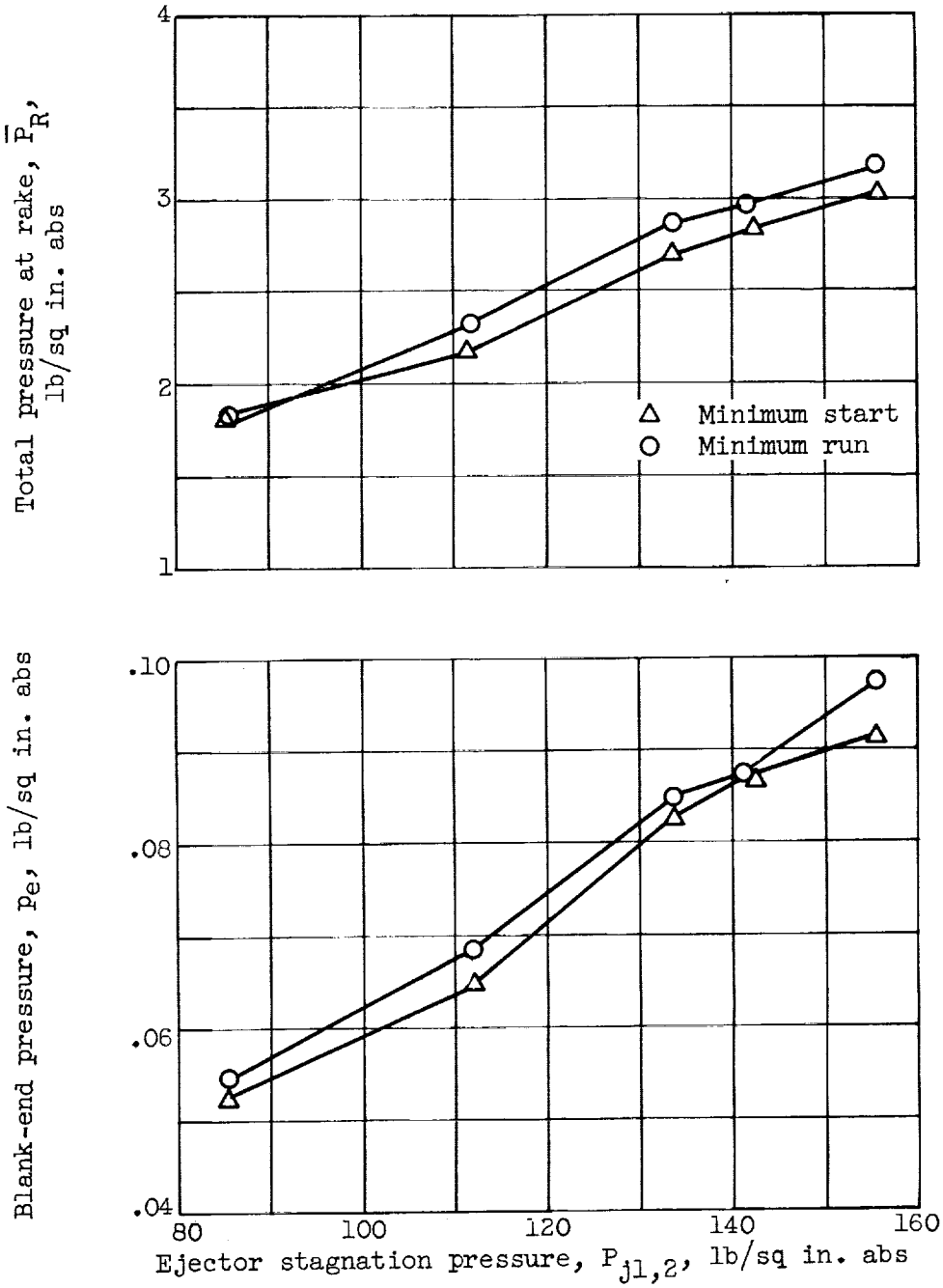

(b) Bleed flow, 0.0016 pound per second; first-stage ejector throat distance, 0.008 inch; short mixer tube.

Figure 7. - Continued. Summary curves. Second-stage ejector throat distance, 0.006 inch.

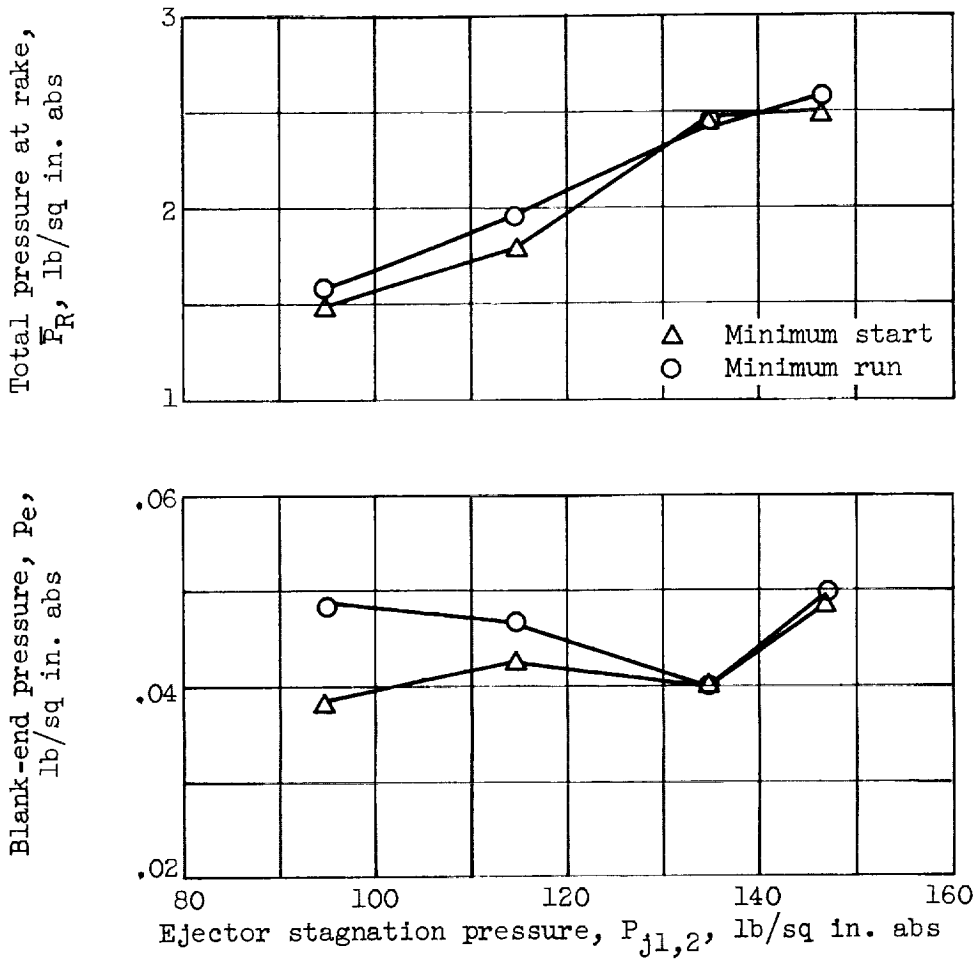

(c) No bleed flow; first-stage ejector throat distance, 0.006 inch; short mixer tube.

Figure 7. - Continued. Summary curves. Second-stage ejector throat distance, 0.006 inch.

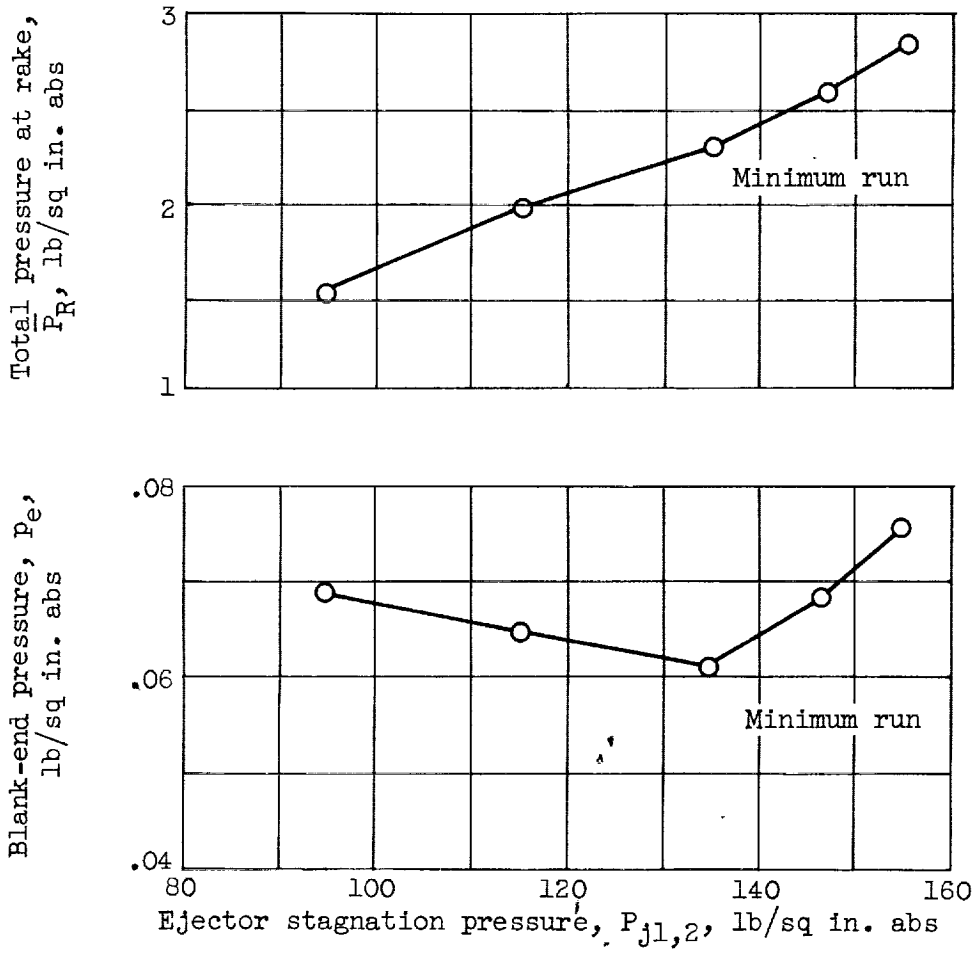

(d) Bleed flow, 0.0016 pound per second; first-stage ejector throat distance, 0.006 inch; short mixer tube.

Figure 7. - Continued. Summary curves. Second-stage ejector throat distance, 0.006 inch.

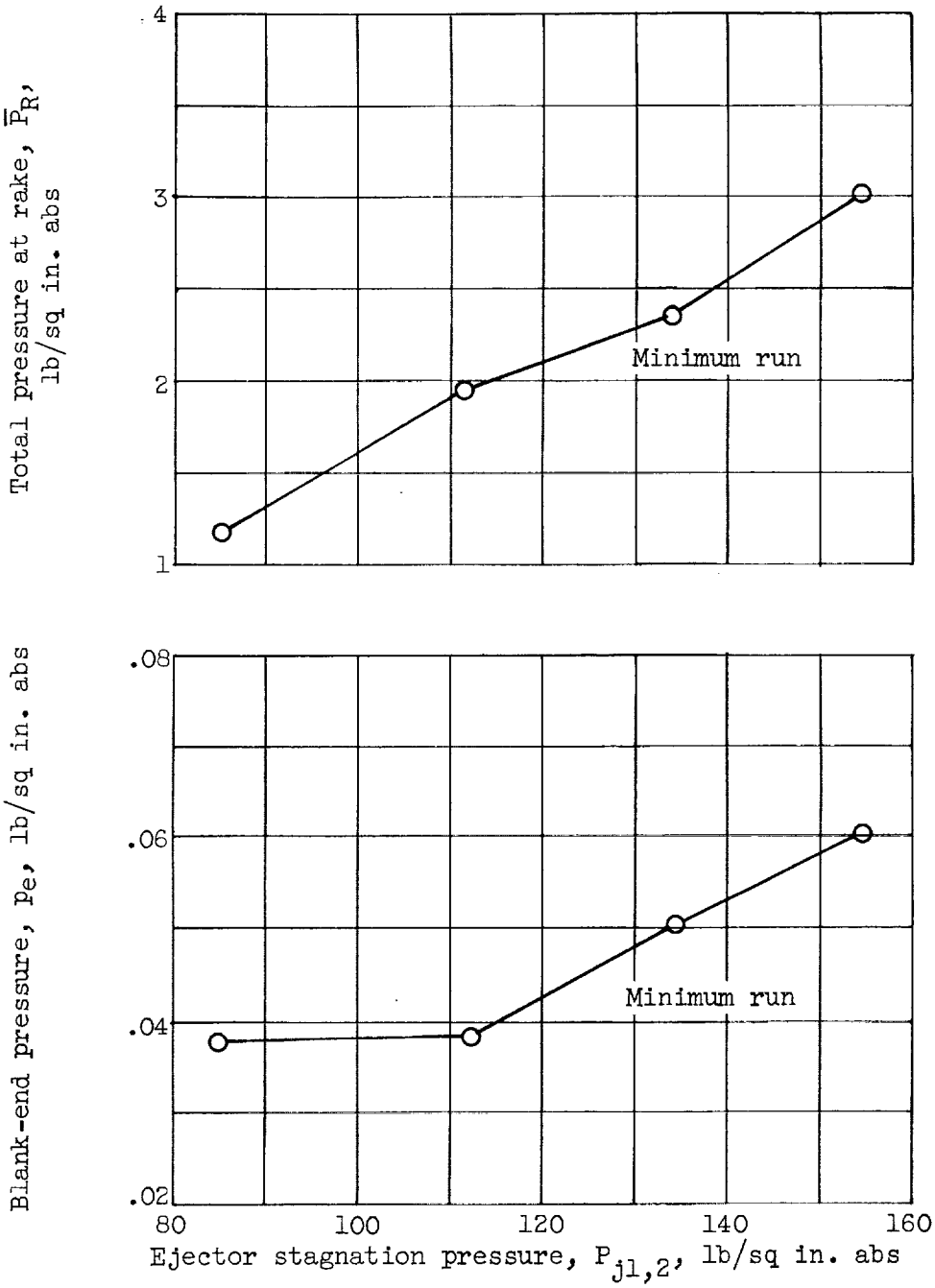

(e) No bleed flow; first-stage ejector throat distance, 0.006 inch; long mixer tube.

Figure 7. - Continued. Summary curves. Second-stage ejector throat distance, 0.006 inch.

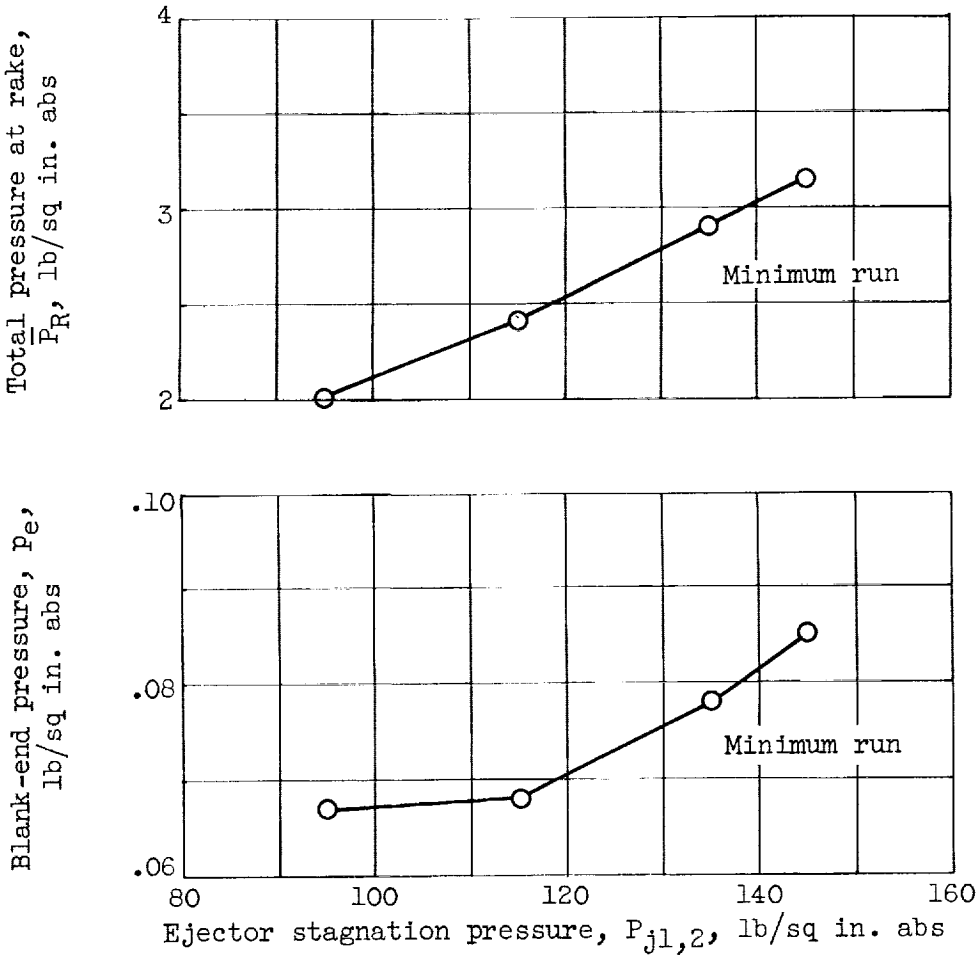

(f) Bleed flow, 0.0016 pound per second; first-stage throat distance, 0.006 inch; long mixer tube.

Figure 7. - Concluded. Summary curves. Second-stage ejector throat distance, 0.006 inch.

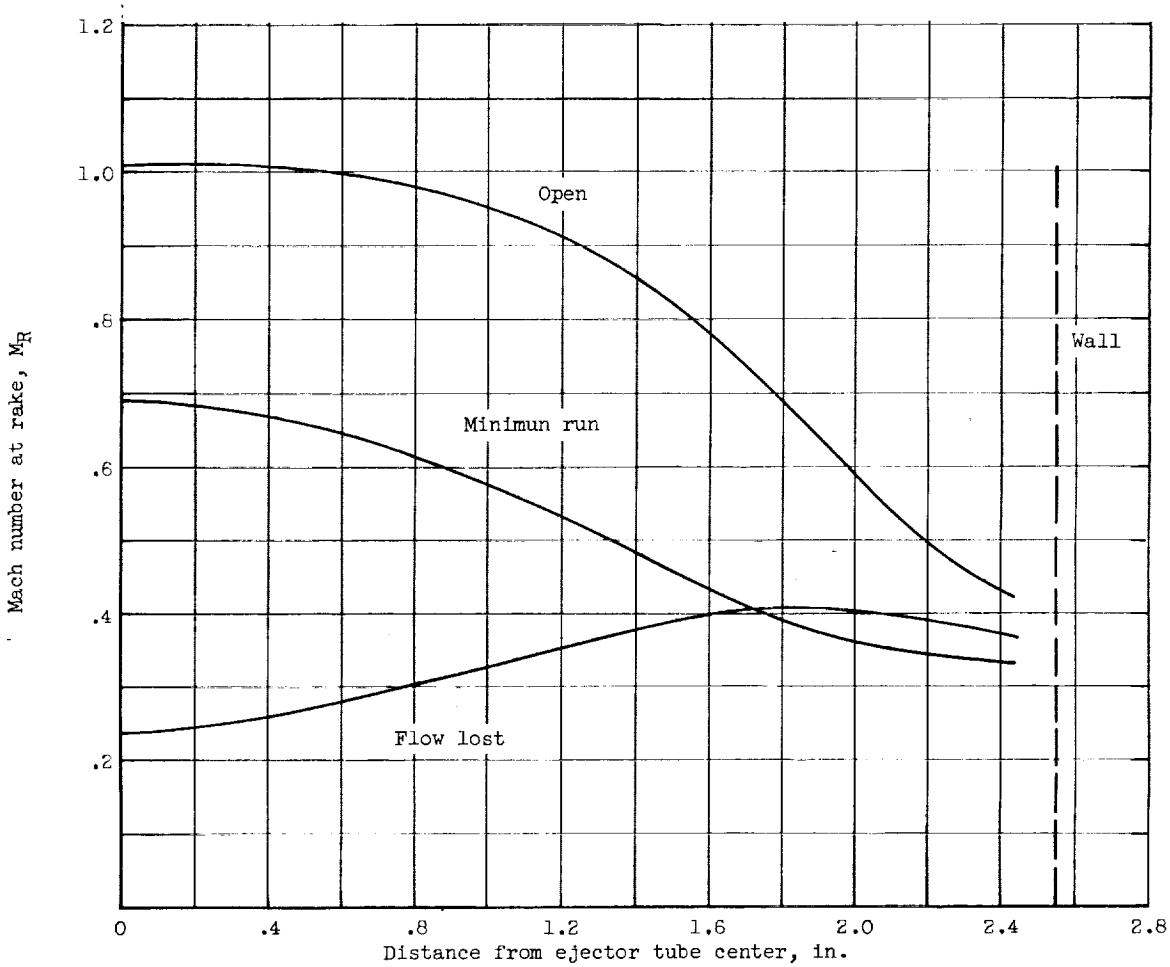

(a) First- and second-stage ejector pressure, 85.5 pounds per square inch absolute; no bleed flow; first-stage ejector mass flow, 0.169 pound per second; second-stage ejector mass flow, 0.167 pound per second; short mixer tube.

Figure 8. - Mach number profiles.

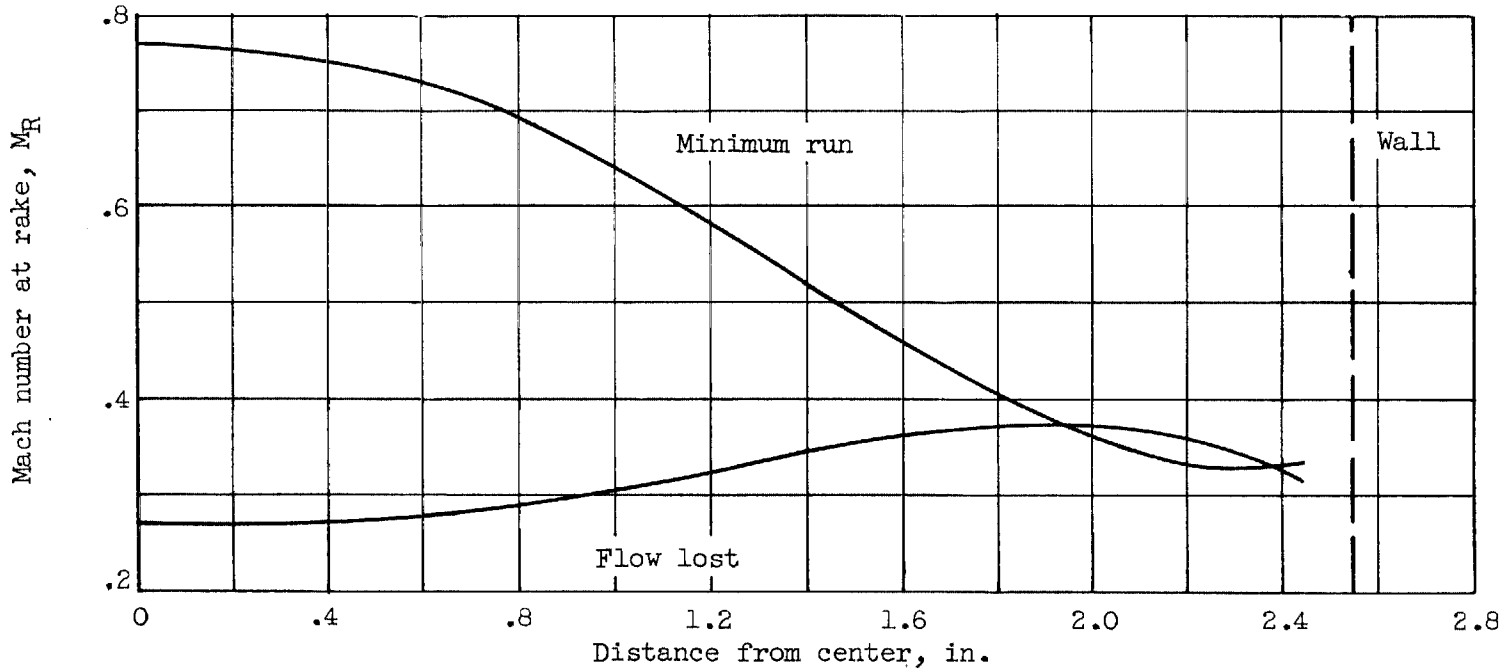

(b) First- and second-stage ejector pressure, 155 pounds per square inch absolute; bleed flow, 0.0016 pound per second; first-stage ejector mass flow, 0.312 pound per second; second-stage ejector mass flow, 0.306 pound per second; short mixer tube.

Figure 8. - Continued. Mach number profiles.

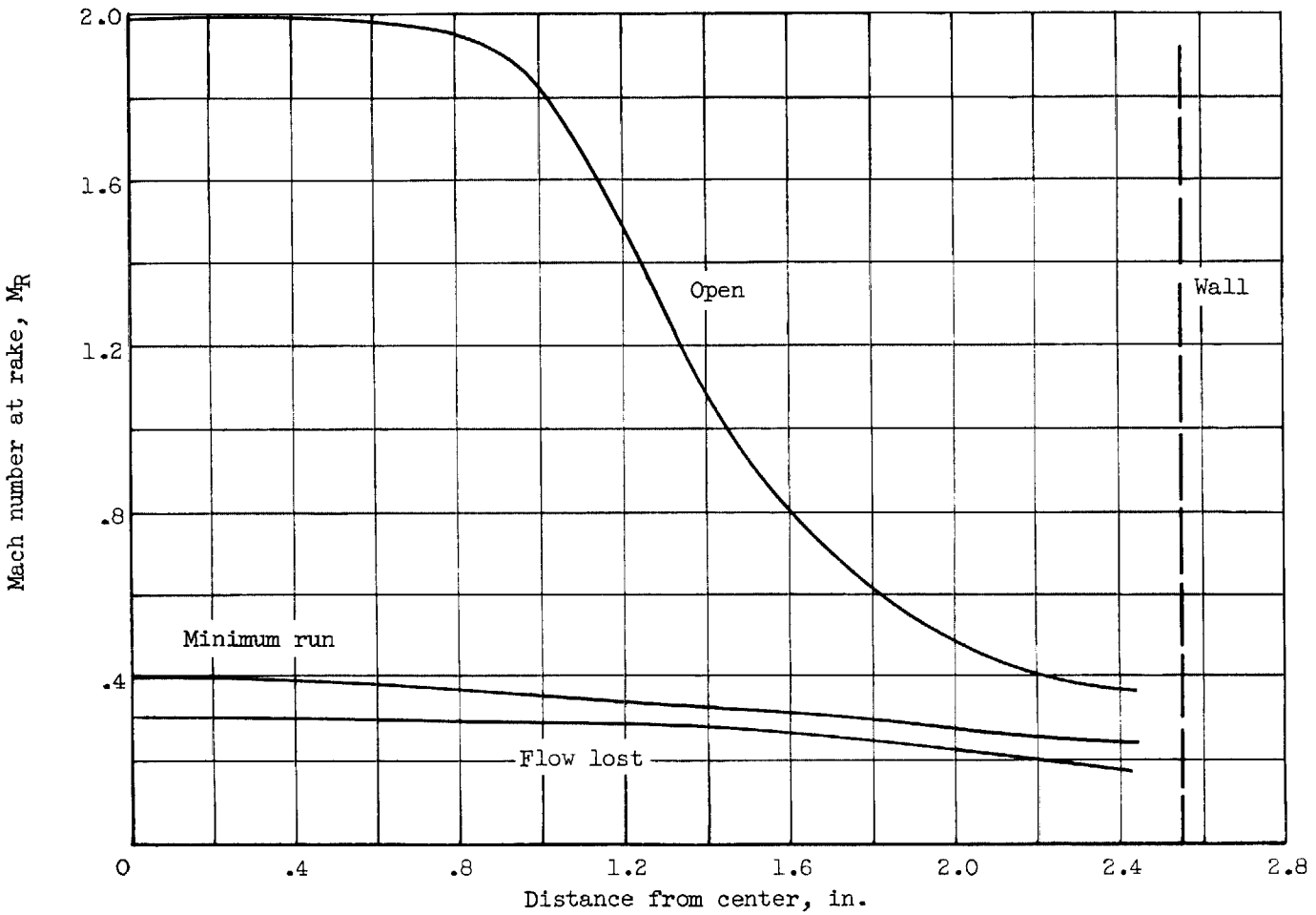

(c) First- and second-stage ejector pressure, 145 pounds per square inch; bleed flow, 0.0016 pound per second; first-stage ejector mass flow, 0.237 pound per second; second-stage mass flow, 0.286 pound per second; long mixer tube.

Figure 8. - Concluded. Mach number profiles.

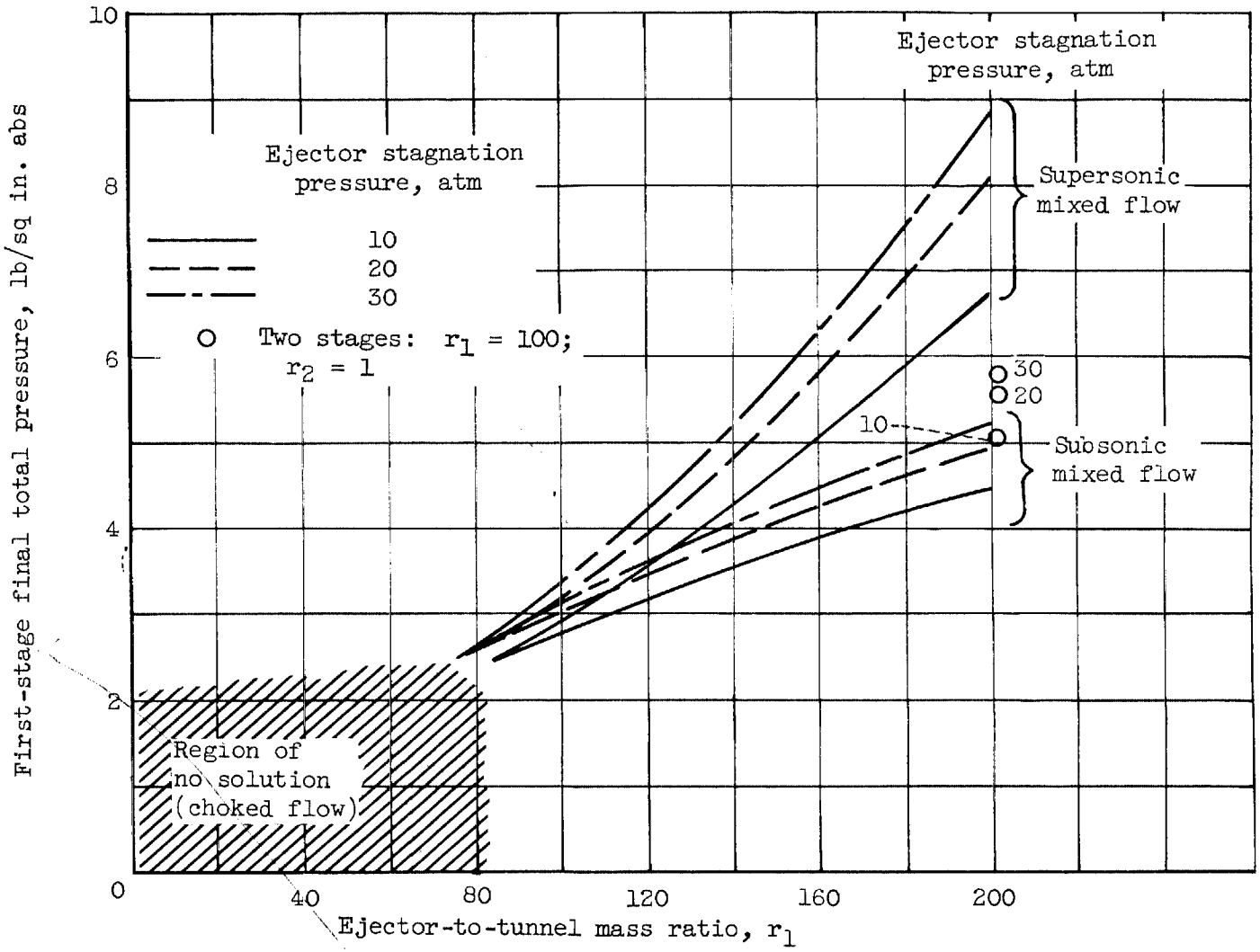

Figure 9. - First-stage ejector operating limits.

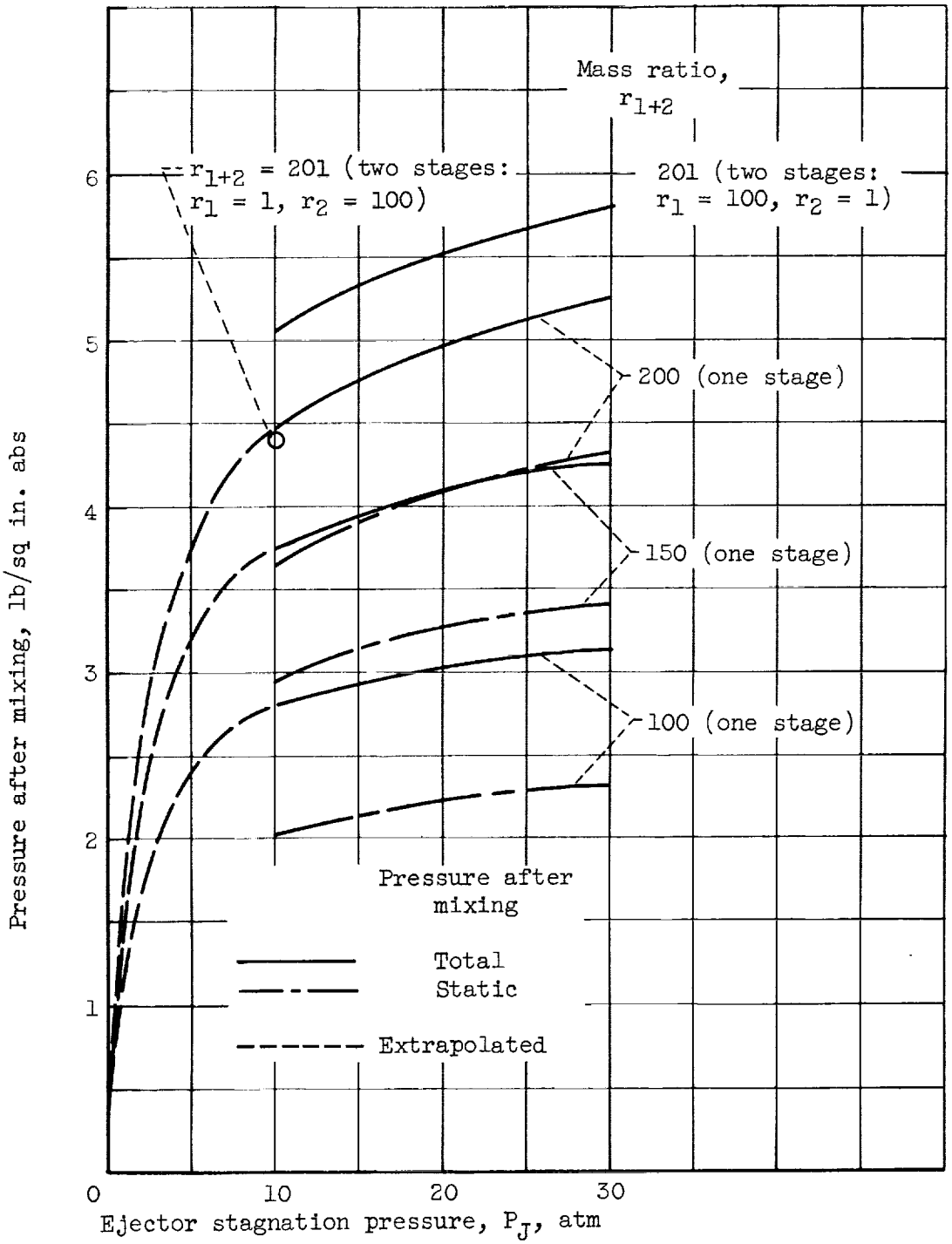

Figure 10. - One- and two-stage ejector performance.

NASA TN D-1215
National Aeronautics and Space Administration.
AN ANALYTICAL AND EXPERIMENTAL EVALUATION OF A TWO-STAGE ANNULAR AIR EJECTOR FOR HIGH-ENERGY WIND TUNNELS. John A. Sheldon and Henry R. Hunczak. June 1962. 35p.
OTS price, $1.00.
(NASA TECHNICAL NOTE D-1215)

An exploratory theoretical evaluation of an annular air ejector-exhauster system for pumping high-energy wind tunnels was made. From the results a 1/8-scale pilot ejector was made and tested. The design parameters were: (1) a first-stage ejector mass-flow ratio of 150, (2) a second-stage ejector mass-flow ratio of 1, and (3) an ejector stagnation pressure of 10 atm. The experimental investigation has confirmed the ability of the ejector to operate between the maximum pressure necessary for starting a typical high-energy tunnel and the minimum pressure required to enable the exhausters to pump the combined tunnel and ejector mass flow.

I. Sheldon, John A.
II. Hunczak, Henry R.
III. NASA TN D-1215

(Initial NASA distribution:
20, Fluid mechanics;
45, Research and development facilities.)

NASA

NASA TN D-1215
National Aeronautics and Space Administration.
AN ANALYTICAL AND EXPERIMENTAL EVALUATION OF A TWO-STAGE ANNULAR AIR EJECTOR FOR HIGH-ENERGY WIND TUNNELS. John A. Sheldon and Henry R. Hunczak. June 1962. 35p.
OTS price, $1.00.
(NASA TECHNICAL NOTE D-1215)

An exploratory theoretical evaluation of an annular air ejector-exhauster system for pumping high-energy wind tunnels was made. From the results a 1/8-scale pilot ejector was made and tested. The design parameters were: (1) a first-stage ejector mass-flow ratio of 150, (2) a second-stage ejector mass-flow ratio of 1, and (3) an ejector stagnation pressure of 10 atm. The experimental investigation has confirmed the ability of the ejector to operate between the maximum pressure necessary for starting a typical high-energy tunnel and the minimum pressure required to enable the exhausters to pump the combined tunnel and ejector mass flow.

I. Sheldon, John A.
II. Hunczak, Henry R.
III. NASA TN D-1215

(Initial NASA distribution:
20, Fluid mechanics;
45, Research and development facilities.)

NASA

NASA TN D-1215
National Aeronautics and Space Administration.
AN ANALYTICAL AND EXPERIMENTAL EVALUATION OF A TWO-STAGE ANNULAR AIR EJECTOR FOR HIGH-ENERGY WIND TUNNELS. John A. Sheldon and Henry R. Hunczak. June 1962. 35p.
OTS price, $1.00.
(NASA TECHNICAL NOTE D-1215)

An exploratory theoretical evaluation of an annular air ejector-exhauster system for pumping high-energy wind tunnels was made. From the results a 1/8-scale pilot ejector was made and tested. The design parameters were: (1) a first-stage ejector mass-flow ratio of 150, (2) a second-stage ejector mass-flow ratio of 1, and (3) an ejector stagnation pressure of 10 atm. The experimental investigation has confirmed the ability of the ejector to operate between the maximum pressure necessary for starting a typical high-energy tunnel and the minimum pressure required to enable the exhausters to pump the combined tunnel and ejector mass flow.

I. Sheldon, John A.
II. Hunczak, Henry R.
III. NASA TN D-1215

(Initial NASA distribution:
20, Fluid mechanics;
45, Research and development facilities.)

NASA

NASA TN D-1215
National Aeronautics and Space Administration.
AN ANALYTICAL AND EXPERIMENTAL EVALUATION OF A TWO-STAGE ANNULAR AIR EJECTOR FOR HIGH-ENERGY WIND TUNNELS. John A. Sheldon and Henry R. Hunczak. June 1962. 35p.
OTS price, $1.00.
(NASA TECHNICAL NOTE D-1215)

An exploratory theoretical evaluation of an annular air ejector-exhauster system for pumping high-energy wind tunnels was made. From the results a 1/8-scale pilot ejector was made and tested. The design parameters were: (1) a first-stage ejector mass-flow ratio of 150, (2) a second-stage ejector mass-flow ratio of 1, and (3) an ejector stagnation pressure of 10 atm. The experimental investigation has confirmed the ability of the ejector to operate between the maximum pressure necessary for starting a typical high-energy tunnel and the minimum pressure required to enable the exhausters to pump the combined tunnel and ejector mass flow.

I. Sheldon, John A.
II. Hunczak, Henry R.
III. NASA TN D-1215

(Initial NASA distribution:
20, Fluid mechanics;
45, Research and development facilities.)

NASA